Title

Osteonecrosis of the jaws (ONJ) in mice after extraction of teeth with periradicular disease.

Authors

Soundia, Akrivoula
Hadaya, Danny
Esfandi, Navid
et al.

Publication Date

2016-09-01

DOI

10.1016/j.bone.2016.06.011

Peer reviewed

HHS Public Access

Author manuscript

Bone. Author manuscript; available in PMC 2017 September 01.

Published in final edited form as:

Bone. 2016 September ; 90: 133–141. doi:10.1016/j.bone.2016.06.011.

Osteonecrosis of the Jaws (ONJ) in Mice after Extraction of Teeth with Periradicular Disease

Akrivoula Soundia[#,1], **Danny Hadaya**[#,1], **Navid Esfandi**[1], **Rafael Scaf de Molon**[1,2], **Olga Bezouglaia**[1], **Sarah M. Dry**[3], **Flavia Q. Pirih**[4], **Tara Aghaloo**[*,1], and **Sotirios Tetradis**[*,1,6]

[1]Division of Diagnostic and Surgical Sciences, UCLA School of Dentistry, Los Angeles, CA 90095, USA

[2]Department of Diagnosis and Surgery, School of Dentistry at Araraquara, Sao Paulo State University, Araraquara 14801–903, Brazil

[3]Department of Pathology and Laboratory Medicine, David Geffen School of Medicine at UCLA, Los Angeles, CA 90095, USA

[4]Division of Constitutive & Regenerative Sciences, UCLA School of Dentistry, Los Angeles, CA 90095, USA

[6]Molecular Biology Institute, UCLA, Los Angeles, CA 90095, USA

Abstract

Osteonecrosis of the jaws (ONJ) is a complication of antiresorptive medications, such as denosumab or bisphosphonates, prescribed to patients with bone malignancy or osteoporosis. The most common instigating local factor in ONJ pathogenesis is tooth extraction. However, in adults the great majority of teeth are extracted due to dental disease. Here, we have investigated alveolar bone healing after extraction of healthy teeth or teeth with naturally occurring periradicular disease in mice treated with high dose zoledronic acid (ZA), a potent bisphosphonate, or OPG-Fc, a RANKL inhibitor. C57BL/6 mice were treated for eight weeks and *in vivo* micro-CT was performed to identify spontaneously occurring periradicular lesions around the roots of maxillary molars. Then, extractions of molars with and without dental disease were performed in all groups.

[*]Corresponding Authors: Sotirios Tetradis DDS, PhD, UCLA School of Dentistry, 10833 Le Conte Ave. CHS Rm. 53-068, Los Angeles, CA 90095-1668, Tel: (310) 825-5712, Fax: (310) 825-7232, stetradis@dentistry.ucla.edu; Tara L. Aghaloo DDS, MD, PhD, UCLA School of Dentistry, 10833 Le Conte Ave. CHS Rm. 53-009, Los Angeles, CA 90095-1668, Tel: (310) 794-7070, Fax: (310) 825-7232, taghaloo@dentistry.ucla.edu.

[#]These authors contributed equally to the manuscript

DISCLOSURES

Dr. Tetradis has served as a paid consultant for and has received grant support from Amgen Inc. All other authors state that they do not have any conflicts of interest.

AUTHOR CONTRIBUTIONS

Study conception and design: AS, DH, NE, RSM, OB, SMD, FQP, TLA, and ST. Data acquisition: AS, DH, NE, RSM, OB, SMD, FQP, TLA, and ST. Data analysis and interpretation: AS, DH, SMD, FQP, TLA, ST. Drafting of manuscript: AS, DH, TLA, and ST. Edition of manuscript: AS, DH, NE, RSM, OB, SMD, FQP, TLA, and ST. All authors were involved in revising the paper critically for important intellectual content, and all authors approved the final version to be published. AS, DH, TLA and ST had full access to all the data in the study and take responsibility for the integrity of the data and the accuracy of the data analysis.

Four weeks later, animals were euthanized and maxillae were dissected and analyzed. Clinically, all vehicle animals with extraction of healthy or diseased teeth, and most OPG-Fc or ZA animals with extraction of healthy teeth showed normal mucosal healing. On the contrary, most animals with OPG-Fc or ZA treatment and extraction of diseased teeth demonstrated impaired healing with visible mucosal defects. Radiographically, bone socket healing was significantly compromised in OPG-Fc and ZA-treated mice with periradicular disease in comparison to other groups. Histologically, all vehicle animals showed normal mucosal healing and socket remodeling. OPG-Fc and ZA animals with extraction of healthy teeth showed normal mucosal healing, woven bone formation in the socket, and decreased remodeling of the original socket confines. OPG-Fc and ZA animals with extraction of diseased teeth showed mucosal defects, persistent prominent inflammatory infiltrate, bone exposure and areas of osteonecrosis. These findings support that dental disease is critical in the pathogenesis of ONJ, not only as the instigating cause for tooth extraction, but also as a compounding factor in ONJ development and pathophysiology.

INTRODUCTION

Medication related osteonecrosis of the jaws (ONJ) is defined as necrotic, exposed bone in the maxillofacial region for at least 8 weeks, in patients on antiresorptive treatment [1, 2] or antiangiogenic medications [2], but without a history of head and neck radiation. Patients with primary bone cancer or metastatic disease on high dose bisphosphonates (BPs), notably zoledronic acid (ZA), or denosumab most commonly suffer from this condition. Patients with osteoporosis or Paget's disease receiving either oral or parenteral antiresorptive medications are at much lower risk [1, 2].

Dentoalveolar surgery is a major local risk factor associated with ONJ incidence, with 52–61% of patients reporting tooth extraction as the precipitating event for clinical manifestation of the disease [3–5]. Based on these clinical observations, ONJ animal models have been developed that combine antiresorptive treatment and extraction of maxillary or mandibular teeth in order to recapitulate clinical, radiographic, and histologic features of the disease [6–12].

The vast majority of teeth in adult patients are extracted due to dental disease [13, 14], which is also true for patients with ONJ [15]. Periodontal or periapical disease, even in the absence of tooth extraction is associated with ONJ occurrence [16] and is considered a local risk factor for the disease [1, 2]. Moreover, improved oral hygiene measures significantly reduce ONJ incidence in patients with multiple myeloma and metastatic cancer [17, 18]. Indeed, we and others have described ONJ models in rodents treated with antiresorptive medications and induced experimental dental disease, without extractions, that capture several attributes of ONJ in patients [19–25]

During these studies, we identified an unexpected model of ONJ in animals with naturally occurring periradicular lesions around the maxillary molar teeth, when they were treated with high doses of ZA or with the RANKL inhibitors RANK-Fc or OPG-Fc. It is noteworthy that no experimental intervention was performed in these animals and the ONJ-like lesions, characterized by periosteal bone apposition, osteonecrosis, severe inflammation and bone exposure, developed spontaneously [24]. Here, taking advantage of this ONJ model, we have

combined the two methodologies of local risk factors (extraction and dental disease), in association with systemic treatment with two different types of antiresorptives, a BP or a RANKL inhibitor, to more closely replicate the clinical setting and investigate ONJ pathogenesis. We have extracted healthy teeth or teeth with natural periradicular lesions in animals treated with vehicle (veh), ZA, or OPG-Fc and have assessed the animals clinically, radiographically, and histologically. Our data indicate that extraction of diseased, but not healthy, teeth is associated with high incidence of ONJ in this mouse model.

MATERIALS AND METHODS

Animal care

Animals were kept and treated according to guidelines of the UCLA Chancellor's Animal Research Committee. Throughout the experimental period, mice were housed in corn-bedding plastic cages (4 mice per cage) in pathogen-free conditions with a light/dark cycle of 12 hours, fed a standard laboratory diet, and given water ad libitum. Fifty seven nine-week-old C57BL/6J male mice (Jackson Laboratory, Bar Harbor, ME, USA), weighing 25g on average (range from 23–28g), were randomly assigned to receive intraperitoneal injections of endotoxin free saline (vehicle), 10 mg/kg OPG-Fc (composed of the RANKL-binding domain of osteoprotegerin linked to the Fc portion of IgG, kindly provided by Amgen Inc, Thousand Oaks, CA), or 200 μg/kg zoledronic acid (ZA) twice a week in morning hours. There were 19 vehicle, 18 OPG-Fc, and 20 ZA treated animals. The antiresorptive doses were chosen in order to induce ONJ in the presence of dental disease, based on our previous studies [22–25]. The protocol followed all recommendations of the ARRIVE (Animal Research: Reporting in Vivo Experiments) guidelines for execution and submission of studies in animals [26].

Animals were treated for eight weeks with vehicle, OPG-Fc or ZA, and then *in vivo* μCT was performed to assess the presence of spontaneous periradicular disease. The study included 6 experimental groups: vehicle, OPG-Fc and ZA treated animals with extraction of either healthy or diseased teeth. Two days after imaging, mice were anesthetized utilizing isoflurane, and maxillary molars from both sides were extracted. For all groups, sites with a fractured buccal cortical plate or fractured teeth during extraction were excluded from subsequent analysis. Four weeks after extractions animals were sacrificed, maxillae were dissected and photographs of the specimens were obtained utilizing a digital optical microscope (Keyence VHX-1000, Osaka, Japan). Then specimens underwent radiographic and histologic assessment, as described below. During *ex vivo* radiographic evaluation, sites with remaining roots were excluded from subsequent analysis. The final study groups consisted of 28, 24 and 25 maxillary sites for vehicle, OPG-Fc or ZA animals respectively.

In vivo μCT scanning

In vivo imaging was performed utilizing the Skyscan 1176 *in vivo* μCT scanner (Bruker Corporation, Belgium) at 18 μm resolution, 50 kVp and 500 μA. Volumetric image data were converted to DICOM format and imported in the Dolphin Imaging software (Chatsworth, CA, USA) to generate 3D and multiplanar reconstructed images. Altered alveolar bone morphology with widening of the periodontal space around the maxillary

molar roots and/or presence of periosteal bone apposition at the alveolar ridge outline were *a priori* considered an indication of periradicular disease.

All scans were de-identified. The presence of periradicular disease was recorded. The distance from the cemento-enamel junction (CEJ) to the alveolar crest (AC) was measured at the distal surface of the second molar, as previously described [24, 25]. Buccal cortical thickness was measured on axial slices oriented parallel to the occlusal plane, in the area of the 2nd molar at the level of the apical third of the roots [24, 25].

ex vivo µCT scanning

Dissected maxillae were imaged by high-resolution *ex vivo* µCT utilizing the SkyScan 1172 µCT scanner (SkyScan, Kontich, Belgium), as described [24, 25]. Volumetric image data were converted to DICOM format and imported in the Dolphin Imaging software to generate 3D and multiplanar reconstructed images, as above.

All scans were de-identified. Healing of extraction sockets was rated as complete (healing of more than 75% of the socket), partial (healing of 25% – 75% of the socket) or absent (healing of less than 25% of the socket). Also, the bone volume (BV), tissue volume (TV), and BV/TV of the alveolar bone excluding the extraction socket were measured, as described [24, 25].

Histology and TRAP staining

Maxillae were fixed for 48 h in 4% paraformaldehyde and then decalcified in 14% EDTA for 3 weeks. Samples were paraffin embedded and 5 µm-thick cross sections were made perpendicular to the long axis of the alveolar ridge at the area of maximum radiographic and clinical changes, as assessed by µCT analysis and clinical photographs. H&E stained slides were digitally scanned utilizing the Aperio AT automated slide scanner and automated image analysis was performed using the Aperio Image Scope software (Aperio Technologies, Inc., Vista, CA, USA). The area of the alveolar bone, from the alveolar crest to the floor of the nasal cavity was defined as the region of interest (ROI). The total number of osteocytic lacunae, the number of empty lacunae, and the surface of osteonecrotic area(s) were quantified. An area of osteonecrosis was defined as a loss of more than five osteocytes with confluent areas of empty lacunae [20, 24, 25]. Lacunae housing necrotic, karyolitic osteocytes, indicated by eosinophilic stained nuclei, were counted as empty osteocytes. The shortest distance from the inferior part of the epithelium to the alveolar crest was measured. If the bone was extruding above the epithelium, in animals with bone exposure, the distance was recorded as negative (Supplemental Fig 1). The Aperio Image Scope software was used to quantify the total bone area, the surface area of osteonecrosis and to make all linear measurements. All histology and digital imaging was performed at the Translational Pathology Core Laboratory (TPCL) at the David Geffen School of Medicine at UCLA.

For enumeration of osteoclasts, tartrate-resistant acid phosphatase (TRAP) staining was performed utilizing the leukocyte acid phosphatase kit (387A-IKT Sigma Aldrich, St. Louis, MO, USA). Positive cells were identified as multinucleated (≥2) TRAP-positive cells in contact with or very close proximity to the bone surface, in the ROI and were counted manually (AS).

Statistics

Raw data were analyzed using the GraphPad Prism Software (GraphPad Software, Inc. La Jolla, CA). Descriptive statistics were used to calculate the mean and the standard error of the mean (SEM). Data were analyzed by a two-way ANOVA and post-hoc Tukey's test for multiple comparisons among the various groups, with a statistical significance of $p<0.05$. The presence or absence of mucosal defect after tooth extraction and the degree of socket healing (complete, partial or absent) were analyzed using the Fisher's exact test.

RESULTS

Radiographic assessment of spontaneous periradicular bone loss around maxillary molars

In vivo microCT revealed the presence of periradicular bone loss in 12/28, 10/24 and 8/25 maxillary sites of all vehicle, OPG-Fc or ZA animals respectively, with no statistical difference among vehicle, OPG-Fc and ZA groups ($p>0.05$). μCT imaging showed a normal PDL space and alveolar bone in vehicle, OPG-Fc and ZA animals with healthy teeth (Fig 1A, A1, B, B1, C and C1). In contrast, significant alveolar bone loss (white arrows) and increased bone thickness (white arrowheads) were seen around the molar roots of animals with periradicular disease (Fig 1D, D1, E, E1, F, F1). Quantification of radiographic features showed statistically increased bone loss in diseased vs. healthy teeth in all groups (Fig 1G). A common radiographic finding in patients with ONJ is periosteal bone deposition causing alveolar expansion [27]. To quantify potential bone deposition along the buccal maxillary cortex, we measured the thickness of the buccal bone in all six groups. Indeed, buccal cortical thickness increased in the diseased vs. healthy site of ZA and OPG-Fc groups, as well as in the diseased site of the ZA and OPG-Fc groups vs. the diseased site of the vehicle group (Fig 1H).

Clinical assessment of mucosal healing after tooth extraction

Visual inspection showed that four weeks after extraction, the alveolar mucosa healed normally in all vehicle treated animals (Fig 2A and D). Normal soft tissue healing was also present in the majority of mice treated with antiresorptives with extraction of healthy teeth, with only 1 of 14 (7.1%) and 2 of 17 (11.7%) OPG-Fc or ZA animals, respectively, demonstrating soft tissue defects (Fig 2B, C, G). In contrast, 7 of 10 (70 %) of OPG-Fc and 6 of 8 (75%) of ZA animals that had undergone extraction of teeth with periradicular disease showed mucosal defects and the presence of exposed bone in the area of the extraction (Fig 2E and F, blue arrows and 2G).

Radiographic assessment of socket healing after tooth extraction

High-resolution *ex vivo* micro-CT was performed to assess bone architecture of the alveolar ridge after tooth extraction. Vehicle animals, irrespective of extraction of healthy or diseased teeth, demonstrated remodeling of the socket outline and, in the great majority of cases, near complete healing of the extraction socket (Fig 3 A, A1, D, D1, D2, G). OPG-Fc and ZA animals that had undergone extraction of healthy teeth, also displayed some extraction socket healing in nearly all sites (12/13 and 14/15 respectively), with the majority of sockets

(9/14 and 14/15 respectively) showing complete healing (Fig 3 B, B1, C, C1, G). Interestingly, in the antiresorptive but not vehicle treated animals, the original outline of the extraction socket was easily identifiable and the socket healed with a granular, woven-like bone that lacked normal trabecular architecture. In contrast, in OPG-Fc and ZA animals, extraction sockets of diseased teeth showed overall decreased healing compared to socket of extracted healthy teeth (Fig 3 G), with several animals showing absence (5/10 and 5/8 respectively) of intra-socket bone formation as seen by multiplanar views (Fig 3 E, E2, F, F2) and 3D rendering (Fig 3 E1, F1, black arrows). Occasional bony spicules were also noted within the empty extraction sockets (Fig 3 F, F2, white arrows). As expected, OPG-Fc and ZA animals demonstrated increased BV/TV values of the alveolar ridge, compared to vehicle animals, without any difference between sites of healthy vs. diseased teeth (Fig 3H).

Histologic assessment of socket healing after tooth extraction

After μCT assessment, histologic evaluation of the maxillae was performed (Fig 4). Vehicle animals with extraction of healthy teeth showed normal healed epithelium (Fig 4A, white arrow) with presence of rete pegs, fibrous connective tissue with no significant inflammatory infiltrate, and remodeled extraction sockets (Fig 4A, A1). Animals treated with either OPG-Fc or ZA and with extraction of healthy teeth also showed normal soft tissue healing, including a regular epithelial lining with the presence of rete pegs (Fig 4B, C, white arrows) and fibrous connective tissue without a significant inflammatory infiltrate. Dense woven bone occupied most of the extraction socket, while the boundaries of the original extraction socket could be easily recognized (Fig 4, B, B1, C, C1).

Vehicle animals with extraction of diseased teeth also showed mostly normal epithelial lining (Fig 4D, white arrow). The underlying connective tissue contained a mild inflammatory infiltrate. In the healing extraction socket, woven bone with multiple reversal lines, and marrow fibrosis were noted (Fig 4D, D1, D2, D3). In OPG-Fc or ZA animals with extraction of diseased teeth (Fig 4E, E1, E2, E3, F, F1, F2, F3), epithelial migration (black arrows) and abundant inflammatory infiltrate (green arrows) in both the epithelial and connective tissue compartments were noted. In several specimens, the extraction socket had not healed with any bone and was not covered by epithelium or connective tissue, but was exposed to the oral cavity (blue arrows).

In other specimens, an epithelial defect was present, and thin fragmented connective tissue, and foreign material debris covered the extraction sockets (orange arrows). Osteonecrosis (Fig 4 E, E1, E2, E3, F, F1, F2, F3 yellow arrows) of the alveolar bone and occasional small sequestra (light blue arrows) were noted.

Quantification of the histologic findings revealed a statistically significant increase in the number of empty osteocytic lacunae and in the osteonecrotic area in OPG-Fc and ZA animals with extraction of diseased teeth compared to extraction of healthy teeth in the same treatment group or compared to extraction of diseased teeth in vehicle animals (Fig 5 A and B). Also, OPG-Fc vs. ZA animals with extraction of diseased teeth showed a higher number of empty osteocytic lacunae and osteonecrotic area (Fig 5 A and B).

Epithelium to alveolar bone crest distance was similar in vehicle animals with extraction of healthy or diseased teeth and in OPG-Fc and ZA animals with extraction of healthy teeth. However, in some OPG-Fc and ZA animals with extraction of diseased teeth, the epithelial to alveolar bone crest distance decreased and in animals with bone exposure it assumed a negative value. This was presumably due to the epithelial migration in combination with inhibition of alveolar bone crest resorption (Fig 5C).

TRAP staining was performed to evaluate osteoclast numbers (Fig 5D). As expected, high numbers of osteoclasts were present in vehicle animals with extraction of healthy teeth, and statistically higher numbers in vehicle animals with extraction of diseased teeth. OPG-Fc treatment inhibited formation of osteoclasts in all animals. As previously observed [23–25], TRAP+ cells in ZA treated animals were atypical, with a round shape and pyknotic nuclear morphology that were detached from the bone surface (not shown). Significantly increased numbers of these atypical TRAP+ cells were seen in animals with extraction of diseased vs. healthy teeth.

DISCUSSION

Major progress has been made in the understanding of ONJ pathophysiologic mechanisms since the disease was first reported more than a decade ago [28, 29]. However, significant gaps in our knowledge still exist [1]. A strategy towards bridging these gaps is the concerted effort of research groups in developing animal models that closely mimic ONJ presentation in humans [30]. For these models, animals are treated systemically with high-dose antiresorptives in combination with a local intervention.

Two approaches to induce changes to the local oral environment and precipitate ONJ development have been utilized [1, 30, 31]. One approach involves tooth extraction [6–12], prompted by well-established observations in clinical studies that clearly associate ONJ with tooth extractions [3–5]. These models employ extraction of healthy teeth in combination with antiresorptives. However, in adult patients, more than 90% of teeth are extracted due to severe dental disease, including periodontitis, extensive caries, periapical disease, root fracture, or failed endodontic treatment [13, 14]. Severe dental disease, as the precipitating factor leading to extraction, also occurs in patients on antiresorptives who eventually develop ONJ [15]. Patients with bone cancer or osteoporosis would not be candidates for elective extraction of healthy teeth. This raises the concern that animal models of ONJ with extraction of healthy teeth might not fully capture the clinical setting of patients with extraction of teeth so severely affected by dental disease that they cannot be managed through conservative interventions.

A second approach in introducing local risk factors for ONJ development in animals utilizes induction of severe dental disease [20–25]. This approach was prompted by the association of periodontal or periapical disease with ONJ in patients in the absence of tooth extraction [1, 2, 16, 32]. An additional revealing observation was the 1981 publication by Gotcher and Jee, reporting the presence of exposed alveolar bone trabeculae protruding into the oral cavity or well into the oral epithelium of rice rats with periodontitis treated with dichloromethylene diphosphonate (Cl_2MDP) [19]. Thus, the authors effectively reported the

development of experimental ONJ nearly 22 years before the disease was reported in patients [28, 29]. However, these dental disease models do not reflect the most common presentation of ONJ in patients, which is a non-healing socket after tooth extraction [1, 2, 15].

The need to more accurately reflect the clinical reality has led researchers to continue developing and improving animal models [1, 30, 31]. In this effort, here we have combined the two approaches of altering the local oral environment to favor ONJ development along with extraction of both healthy and diseased teeth. Additionally, animals were treated with two different classes of antiresorptives: ZA, a potent BP, or OPG-Fc, a RANKL inhibitor. We confirmed the presence of dental disease prior to tooth extractions by performing *in vivo* microCT and radiographically assessing the architecture of the periodontal bone and the alveolar ridge. The incidence of dental disease was comparable in all groups, as reported in our previous publication [24]. Bone loss and cortical bone thickness prior to tooth extraction, as assessed by *in vivo* microCT, were similar to our previous report [24]. However, the current data expand our previous study and provide visual, radiographic and histologic assessment of the socket healing after extraction of healthy vs. diseased teeth in vehicle vs. antiresorptive treated animals.

Mucosa healed normally after extraction of healthy or diseased teeth in vehicle animals, and following extraction of healthy teeth in animals treated with antiresorptives. In contrast, extraction of diseased teeth in animals treated with antiresorptives resulted in mucosal defects resembling clinical ONJ in 70–75% of the sites. Our previous study in the absence of tooth extraction, reported bone exposure in 36.4–52% of diseased teeth in animals on antiresorptives. Importantly, in that publication, bone exposure was noted only histologically and not with visual inspection [24]

Radiographic assessment of the extraction socket revealed normal healing of all the sockets in vehicle animals with extraction of healthy or diseased teeth. In OPG-Fc or ZA animals with extraction of healthy teeth, the extraction sockets healed mostly with woven bone that was distinct from the remaining alveolar bone. However, in the same animal groups, but with extraction of diseased teeth, 50–60% of the animals showed defective socket healing with occasional sequestration.

Interestingly, quantitative histologic measures, including osteonecrotic area, number of empty osteocytic lacunae and epithelial to alveolar bone crest distance were similar between the current data and our previous report [24], suggesting that although tooth extraction affected mucosal healing and socket remodeling, it did not affect the extent of osteonecrosis. These observations support the thesis that bone necrosis precedes mucosal defect and do not favor the hypothesis of a direct impairment of mucosal integrity by antiresorptive treatments [33].

Our findings closely parallel the clinical, radiographic, and histologic features of ONJ in patients with exposed and necrotic bone, without (Stage 1) or with (Stage 2) evidence of infection [1, 2]. Interestingly, we did not observe any animals with extensive changes of the alveolar bone structure, pathologic fractures, extraoral fistulae, or oronasal communication

that would be classified as Stage 3 ONJ. The absence of such severely affected animals is possibly due to the short duration of our experiments, the lower incidence of Stage 3 ONJ compared to other stages [34–36], or the lack of a concomitant systemic factor that would compound healing of the oral tissues [1, 2].

Surprisingly, very few animals with extraction of healthy teeth and treated with antiresorptives presented with mucosal defects or radiographic and histologic features resembling ONJ. This finding appears in agreement with some, but not all, published studies that have utilized extraction of healthy teeth in animals on BP or other antiresorptive treatment. Indeed, the reported outcomes of disease incidence and severity in ONJ rodent extraction models vary considerably [30]. This variability has been hypothesized to be due to the type, route of administration, and dose regimen of BP delivery, in combination with the lack of well-defined outcome measures that define the presence of ONJ in rodents [30]. It is noteworthy, that studies consistently reporting ONJ-like features in mice or rat extraction models include in their experimental design systemic risk factors such as steroid or chemotherapy treatment, vitamin D deficiency, or diabetes all of which alter soft tissue and/or bone homeostasis and compound wound healing [6–8, 10, 12, 37–39].

Our results here point to an additional factor contributing to the variability of ONJ incidence and severity in animal model studies that lack a concomitant systemic risk factor [9, 11, 40–46]. In our experience, occurrence of spontaneous periradicular lesions around maxillary teeth in C57Bl/6J or DBA1/J male mice ranges from 35–50% [24], varies among vendor shipment of animals, and is unavoidable. The only way to predictably affirm the presence or absence of changes in alveolar bone is to perform *in vivo* microCT prior to tooth extraction, as performed in our present studies. Thus, it is plausible that in some studies, extractions could have involved diseased teeth that might have inadvertently escaped detection. Based on our data presented herein, such extractions in animals under antiresorptive treatment would likely present with clinical, radiographic, and histologic features of ONJ-like lesions.

In our studies, OPG-Fc vs. ZA animals showed a significantly larger number of empty osteocytic lacunae and osteonecrotic area, suggesting that the extent of osteonecrosis might be slightly greater after OPG-Fc treatment. We had made a similar observation of higher number of empty osteocytic lacunae with OPG-Fc vs. ZA treatment previously [24]. This finding could be within expected experimental variation. However, it could also reflect diverse residual osteoclastic activity after treatment with the two antiresorptives. Indeed, OPG-Fc abolished formation of osteoclastic cells, suggesting complete inhibition of bone resorption. On the other hand, TRAP positive cells were present in the ZA animals, but demonstrated an altered morphology. Thus, some degree of bone resorption must have occurred that caused ZA release from the bone matrix and subsequent intracellular translocation to induced alterations in osteoclast function and morphology. Nevertheless, it is important to note that both OPG-Fc and ZA animals presented similar incidence of mucosal defects and extraction socket healing deficits.

From a clinical point of view, our studies demonstrate the importance of detailed radiographic assessment of bone changes prior to tooth extraction in patients on antiresorptive treatment. Indeed, the most recent International Consensus paper [1]

recommends that in patients for whom ONJ is a clinical concern and teeth extractions are considered, small field of view (FOV), high resolution Cone Beam Computed Tomography (CBCT) or multi-detector CT scans are recommended, if available. These imaging modalities provide valuable information on changes in cortical and trabecular architecture, periosteal reaction, osteolysis, or sequestration.

In conclusion, we have created an approach that refines existing ONJ mouse models to more closely parallel the clinical setting. We report that extraction of diseased, but not of healthy teeth in mice treated with high-dose antiresorptives led to mucosal defects, and radiographic and histologic features of ONJ. Our data, in association with previous published reports, strongly suggest that dental disease is critical in pathogenesis of ONJ, not only as the instigating cause for tooth extraction, but also as a compounding factor in ONJ development.

Supplementary Material

Refer to Web version on PubMed Central for supplementary material.

Acknowledgments

This work was supported by grant support from Amgen Inc (ST), and by NIH/NIDCR DE019465 (ST). Danny Hadaya was supported by T90/R90 DE007296.

References

1. Khan A, Morrison A, Hanley D, Felsenberg D, McCauley L, O'Ryan F, Reid I, Ruggiero S, Taguchi A, Tetradis S, Watts N, Brandi M, Peters E, Guise T, Eastell R, Cheung A, Morin S, Masri B, Cooper C, Morgan S, Obermayer-Pietsch B, Langdahl B, Al Dabagh R, Davison K, Kendler D, Sandor G, Josse R, Bhandari M, El Rabbany M, Pierroz D, Sulimani R, Saunders D, Brown J, Compston J, J. behalf of the International Task Force on Osteonecrosis of the. Diagnosis and Management of Osteonecrosis of the Jaw: A Systematic Review and International Consensus. J Bone Miner Res. 2014
2. Ruggiero, SL., Dodson, TB., Fantasia, J., Goodday, R., Aghaloo, T., Mehrotra, B., O'Ryan, F. Medication-Related Osteonecrosis of the Jaw-2014 Update. 2014. http://www.aaoms.org/docs/position_papers/mronj_position_paper.pdf?pdf=MRONJ-Position-Paper
3. Vahtsevanos K, Kyrgidis A, Verrou E, Katodritou E, Triaridis S, Andreadis CG, Boukovinas I, Koloutsos GE, Teleioudis Z, Kitikidou K, Paraskevopoulos P, Zervas K, Antoniades K. Longitudinal cohort study of risk factors in cancer patients of bisphosphonate-related osteonecrosis of the jaw. J Clin Oncol. 2009; 27(32):5356–62. [PubMed: 19805682]
4. Fehm T, Beck V, Banys M, Lipp HP, Hairass M, Reinert S, Solomayer EF, Wallwiener D, Krimmel M. Bisphosphonate-induced osteonecrosis of the jaw (ONJ): Incidence and risk factors in patients with breast cancer and gynecological malignancies. Gynecol Oncol. 2009; 112(3):605–9. [PubMed: 19136147]
5. Saad F, Brown JE, Van Poznak C, Ibrahim T, Stemmer SM, Stopeck AT, Diel IJ, Takahashi S, Shore N, Henry DH, Barrios CH, Facon T, Senecal F, Fizazi K, Zhou L, Daniels A, Carriere P, Dansey R. Incidence, risk factors, and outcomes of osteonecrosis of the jaw: integrated analysis from three blinded active-controlled phase III trials in cancer patients with bone metastases. Ann Oncol. 2012; 23(5):1341–7. [PubMed: 21986094]
6. Sonis ST, Watkins BA, Lyng GD, Lerman MA, Anderson KC. Bony changes in the jaws of rats treated with zoledronic acid and dexamethasone before dental extractions mimic bisphosphonate-related osteonecrosis in cancer patients. Oral Oncol. 2009; 45(2):164–72. [PubMed: 18715819]

7. Hokugo A, Christensen R, Chung EM, Sung EC, Felsenfeld AL, Sayre JW, Garrett N, Adams JS, Nishimura I. Increased prevalence of bisphosphonate-related osteonecrosis of the jaw with vitamin D deficiency in rats. J Bone Miner Res. 2010; 25(6):1337–49. [PubMed: 20200938]

8. Bi Y, Gao Y, Ehirchiou D, Cao C, Kikuiri T, Le A, Shi S, Zhang L. Bisphosphonates cause osteonecrosis of the jaw-like disease in mice. Am J Pathol. 2010; 177(1):280–90. [PubMed: 20472893]

9. Abtahi J, Agholme F, Sandberg O, Aspenberg P. Bisphosphonate-induced osteonecrosis of the jaw in a rat model arises first after the bone has become exposed. No primary necrosis in unexposed bone. J Oral Pathol Med. 2012; 41(6):494–9. [PubMed: 22268631]

10. Kuroshima S, Yamashita J. Chemotherapeutic and antiresorptive combination therapy suppressed lymphangiogenesis and induced osteonecrosis of the jaw-like lesions in mice. Bone. 2013; 56(1): 101–9. [PubMed: 23727433]

11. Williams DW, Lee C, Kim T, Yagita H, Wu H, Park S, Yang P, Liu H, Shi S, Shin KH, Kang MK, Park NH, Kim RH. Impaired Bone Resorption and Woven Bone Formation Are Associated with Development of Osteonecrosis of the Jaw-Like Lesions by Bisphosphonate and Anti-Receptor Activator of NF-kappaB Ligand Antibody in Mice. Am J Pathol. 2014; 184(11):3084–93. [PubMed: 25173134]

12. Zhang Q, Yu W, Lee S, Xu Q, Naji A, Le AD. Bisphosphonate Induces Osteonecrosis of the Jaw in Diabetic Mice via NLRP3/Caspase-1-Dependent IL-1beta Mechanism. J Bone Miner Res. 2015; 30(12):2300–12. [PubMed: 26081624]

13. Phipps KR V, Stevens J. Relative contribution of caries and periodontal disease in adult tooth loss for an HMO dental population. J Public Health Dent. 1995; 55(4):250–2. [PubMed: 8551465]

14. Chrysanthakopoulos NA. Reasons for extraction of permanent teeth in Greece: a five-year follow-up study. Int Dent J. 2011; 61(1):19–24. [PubMed: 21382029]

15. Marx, RE. Oral and Intravenous Bisphosphonate Induced Osteonecrosis of the Jaws: History, Etiology, Prevention and Treatment. 2nd. Quintessence Pub Co; 2011.

16. Marx RE, Sawatari Y, Fortin M, Broumand V. Bisphosphonate-induced exposed bone (osteonecrosis/osteopetrosis) of the jaws: risk factors, recognition, prevention, and treatment. J Oral Maxillofac Surg. 2005; 63(11):1567–75. [PubMed: 16243172]

17. Ripamonti CI, Maniezzo M, Campa T, Fagnoni E, Brunelli C, Saibene G, Bareggi C, Ascani L, Cislaghi E. Decreased occurrence of osteonecrosis of the jaw after implementation of dental preventive measures in solid tumour patients with bone metastases treated with bisphosphonates. The experience of the National Cancer Institute of Milan. Ann Oncol. 2009; 20(1):137–45.

18. Dimopoulos MA, Kastritis E, Bamia C, Melakopoulos I, Gika D, Roussou M, Migkou M, Eleftherakis-Papaiakovou E, Christoulas D, Terpos E, Bamias A. Reduction of osteonecrosis of the jaw (ONJ) after implementation of preventive measures in patients with multiple myeloma treated with zoledronic acid. Ann Oncol. 2009; 20(1):117–20. [PubMed: 18689864]

19. Gotcher JE, Jee WS. The progress of the periodontal syndrome in the rice cat. II. The effects of a diphosphonate on the periodontium. J Periodontal Res. 1981; 16(4):441–55. [PubMed: 6459441]

20. Aghaloo TL, Kang B, Sung EC, Shoff M, Ronconi M, Gotcher JE, Bezouglaia O, Dry SM, Tetradis S. Periodontal disease and bisphosphonates induce osteonecrosis of the jaws in the rat. J Bone Miner Res. 2011; 26(8):1871–82. [PubMed: 21351151]

21. Aguirre JI, Akhter MP, Kimmel DB, Pingel JE, Williams A, Jorgensen M, Kesavalu L, Wronski TJ. Oncologic doses of zoledronic acid induce osteonecrosis of the jaw-like lesions in rice rats (Oryzomys palustris) with periodontitis. J Bone Miner Res. 2012; 27(10):2130–43. [PubMed: 22623376]

22. Kang B, Cheong S, Chaichanasakul T, Bezouglaia O, Atti E, Dry SM, Pirih FQ, Aghaloo TL, Tetradis S. Periapical disease and bisphosphonates induce osteonecrosis of the jaws in mice. J Bone Miner Res. 2013; 28(7):1631–40. [PubMed: 23426919]

23. Aghaloo TL, Cheong S, Bezouglaia O, Kostenuik P, Atti E, Dry SM, Pirih FQ, Tetradis S. RANKL inhibitors induce osteonecrosis of the jaw in mice with periapical disease. J Bone Miner Res. 2014; 29(4):843–54. [PubMed: 24115073]

24. de Molon RS, Cheong S, Bezouglaia O, Dry SM, Pirih F, Cirelli JA, Aghaloo TL, Tetradis S. Spontaneous osteonecrosis of the jaws in the maxilla of mice on antiresorptive treatment: A novel ONJ mouse model. Bone. 2014; 68:11–9. [PubMed: 25093262]
25. de Molon RS, Shimamoto H, Bezouglaia O, Pirih FQ, Dry SM, Kostenuik P, Boyce RW, Dwyer D, Aghaloo TL, Tetradis S. OPG-Fc but Not Zoledronic Acid Discontinuation Reverses Osteonecrosis of the Jaws (ONJ) in Mice. J Bone Miner Res. 2015; 30(9):1627–40. [PubMed: 25727550]
26. Kilkenny C, Browne WJ, Cuthill IC, Emerson M, Altman DG. Improving bioscience research reporting: the ARRIVE guidelines for reporting animal research. Osteoarthritis Cartilage. 2012; 20(4):256–60. [PubMed: 22424462]
27. Arce K, Assael LA, Weissman JL, Markiewicz MR. Imaging findings in bisphosphonate-related osteonecrosis of jaws. J Oral Maxillofac Surg. 2009; 67(5 Suppl):75–84. [PubMed: 19371818]
28. Marx RE. Pamidronate (Aredia) and zoledronate (Zometa) induced avascular necrosis of the jaws: a growing epidemic. J Oral Maxillofac Surg. 2003; 61(9):1115–7. [PubMed: 12966493]
29. Ruggiero SL, Mehrotra B, Rosenberg TJ, Engroff SL. Osteonecrosis of the jaws associated with the use of bisphosphonates: a review of 63 cases. J Oral Maxillofac Surg. 2004; 62(5):527–34. [PubMed: 15122554]
30. Allen MR. Medication-Related Osteonecrosis of the Jaw: Basic and Translational Science Updates. Oral Maxillofac Surg Clin North Am. 2015; 27(4):497–508. [PubMed: 26277349]
31. Aghaloo T, Hazboun R, Tetradis S. Pathophysiology of Osteonecrosis of the Jaws. Oral Maxillofac Surg Clin North Am. 2015; 27(4):489–96. [PubMed: 26412796]
32. Boonyapakorn T, Schirmer I, Reichart PA, Sturm I, Massenkeil G. Bisphosphonate-induced osteonecrosis of the jaws: prospective study of 80 patients with multiple myeloma and other malignancies. Oral Oncol. 2008; 44(9):857–69. [PubMed: 18282788]
33. Reid IR, Bolland MJ, Grey AB. Is bisphosphonate-associated osteonecrosis of the jaw caused by soft tissue toxicity? Bone. 2007; 41(3):318–20. [PubMed: 17572168]
34. Filleul O, Crompot E, Saussez S. Bisphosphonate-induced osteonecrosis of the jaw: a review of 2,400 patient cases. J Cancer Res Clin Oncol. 2010; 136(8):1117–24. [PubMed: 20508948]
35. Vescovi P, Campisi G, Fusco V, Mergoni G, Manfredi M, Merigo E, Solazzo L, Gabriele M, Gaeta GM, Favia G, Peluso F, Colella G. Surgery-triggered and non surgery-triggered Bisphosphonate-related Osteonecrosis of the Jaws (BRONJ): A retrospective analysis of 567 cases in an Italian multicenter study. Oral Oncol. 2011; 47(3):191–4. [PubMed: 21292541]
36. Otto S, Schreyer C, Hafner S, Mast G, Ehrenfeld M, Sturzenbaum S, Pautke C. Bisphosphonate-related osteonecrosis of the jaws - characteristics, risk factors, clinical features, localization and impact on oncological treatment. J Craniomaxillofac Surg. 2012; 40(4):303–9. [PubMed: 21676622]
37. Lopez-Jornet P, Camacho-Alonso F, Molina-Minano F, Gomez-Garcia F, Vicente-Ortega V. An experimental study of bisphosphonate-induced jaws osteonecrosis in Sprague-Dawley rats. J Oral Pathol Med. 2010; 39(9):697–702. [PubMed: 20819131]
38. Kikuiri T, Kim I, Yamaza T, Akiyama K, Zhang Q, Li Y, Chen C, Chen W, Wang S, Le AD, Shi S. Cell-based immunotherapy with mesenchymal stem cells cures bisphosphonate-related osteonecrosis of the jaw-like disease in mice. J Bone Miner Res. 2010; 25(7):1668–79. [PubMed: 20200952]
39. Takaoka K, Yamamura M, Nishioka T, Abe T, Tamaoka J, Segawa E, Shinohara M, Ueda H, Kishimoto H, Urade M. Establishment of an Animal Model of Bisphosphonate-Related Osteonecrosis of the Jaws in Spontaneously Diabetic Torii Rats. PLoS One. 2015; 10(12):e0144355. [PubMed: 26659123]
40. Tsurushima H, Kokuryo S, Sakaguchi O, Tanaka J, Tominaga K. Bacterial promotion of bisphosphonate-induced osteonecrosis in Wistar rats. Int J Oral Maxillofac Surg. 2013; 42(11): 1481–7. [PubMed: 23932020]
41. Dayisoylu EH, Ungor C, Tosun E, Ersoz S, Kadioglu Duman M, Taskesen F, Senel FC. Does an alkaline environment prevent the development of bisphosphonate-related osteonecrosis of the jaw? An experimental study in rats. Oral Surg Oral Med Oral Pathol Oral Radiol. 2014; 117(3):329–34. [PubMed: 24368141]

42. Barba-Recreo P, Del Castillo Pardo de Vera JL, Garcia-Arranz M, Yebenes L, Burgueno M. Zoledronic acid - related osteonecrosis of the jaws. Experimental model with dental extractions in rats. J Craniomaxillofac Surg. 2014; 42(6):744–50. [PubMed: 24342733]

43. Yang H, Pan H, Yu F, Chen K, Shang G, Xu Y. A novel model of bisphosphonate-related osteonecrosis of the jaw in rats. Int J Clin Exp Pathol. 2015; 8(5):5161–7. [PubMed: 26191212]

44. Kobayashi Y, Hiraga T, Ueda A, Wang L, Matsumoto-Nakano M, Hata K, Yatani H, Yoneda T. Zoledronic acid delays wound healing of the tooth extraction socket, inhibits oral epithelial cell migration, and promotes proliferation and adhesion to hydroxyapatite of oral bacteria, without causing osteonecrosis of the jaw, in mice. J Bone Miner Metab. 2010; 28(2):165–75. [PubMed: 19882100]

45. Zandi M, Dehghan A, Malekzadeh H, Janbaz P, Ghadermazi K, Amini P. Introducing a protocol to create bisphosphonate-related osteonecrosis of the jaw in rat animal model. J Craniomaxillofac Surg. 2016; 44(3):271–8. [PubMed: 26805920]

46. Park S, Kanayama K, Kaur K, Tseng HC, Banankhah S, Quje DT, Sayre JW, Jewett A, Nishimura I. Osteonecrosis of the Jaw Developed in Mice: DISEASE VARIANTS REGULATED BY gammadelta T CELLS IN ORAL MUCOSAL BARRIER IMMUNITY. J Biol Chem. 2015; 290(28):17349–66. [PubMed: 26013832]

Highlights

- Extraction of teeth with dental disease for ONJ development in mice is studied.
- Two different kinds of antiresorptives, a RANKL inhibitor or zoledronate were used.
- All vehicle mice with extraction of healthy or diseased teeth healed uneventfully.
- 90% of antiresorptive mice with extracted healthy teeth had normal mucosal healing.
- Most antiresorptive mice with extracted diseased teeth developed ONJ lesions.

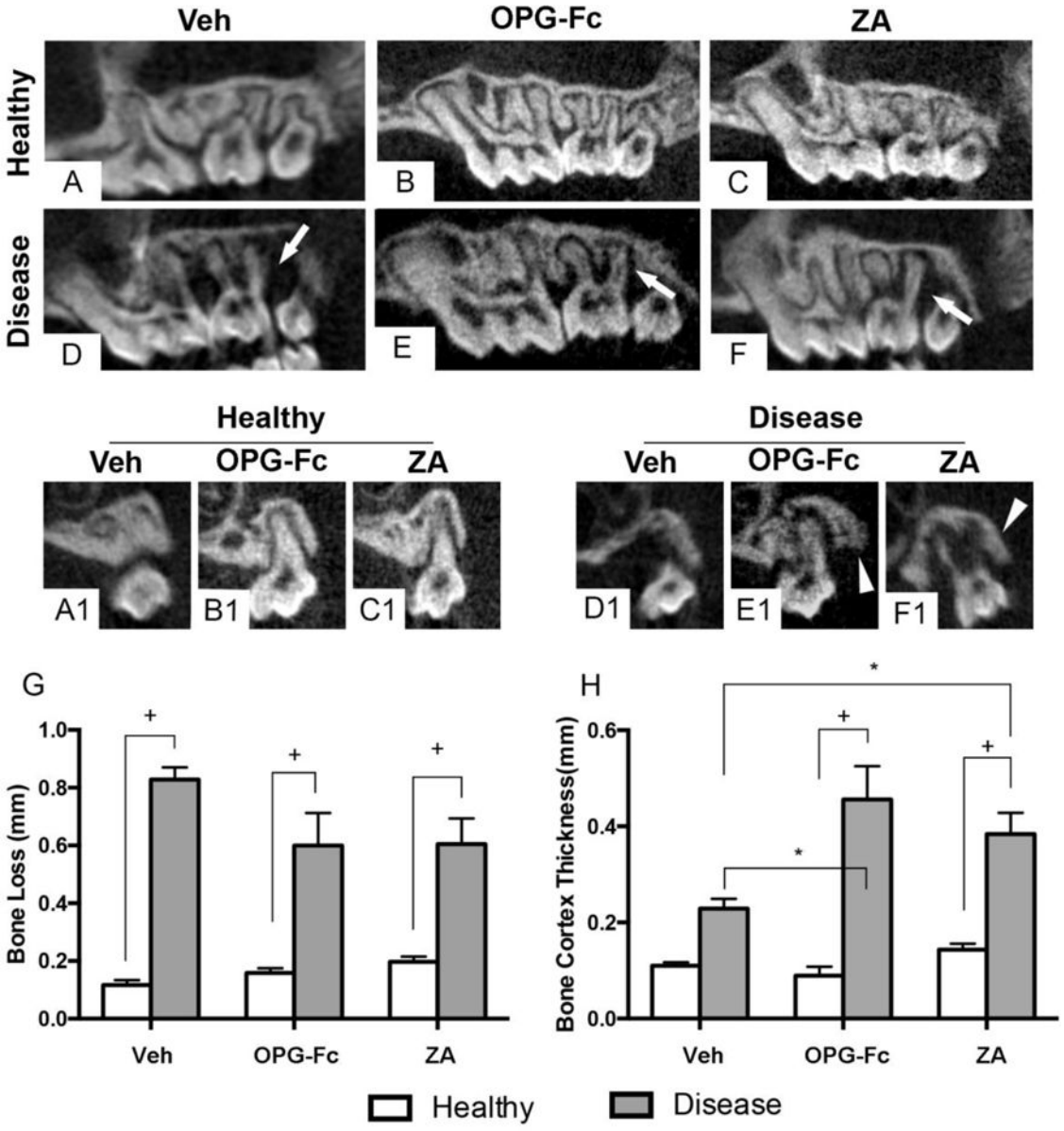

Figure 1. ***In-vivo*** **µCT assessment of the maxillary molars prior to tooth extraction**

(A, B, C) Sagittal and (A1, B1, C1) coronal sections of sites with healthy molars in vehicle, OPG-Fc, and ZA groups, respectively. (D–F) Sagittal and (D1-F1) coronal sections of sites with diseased molars in vehicle, OPG-Fc, and ZA groups, respectively. Quantification of (G) interproximal bone loss and (H) buccal cortex thickness. + Statistically significantly different, $p < 0.0001$. *Statistically significant difference among compared groups, $p < 0.05$. Differences among groups were calculated by two-way ANOVA and post-hoc Tukey's test for multiple comparisons. Data represent the mean ± SEM.

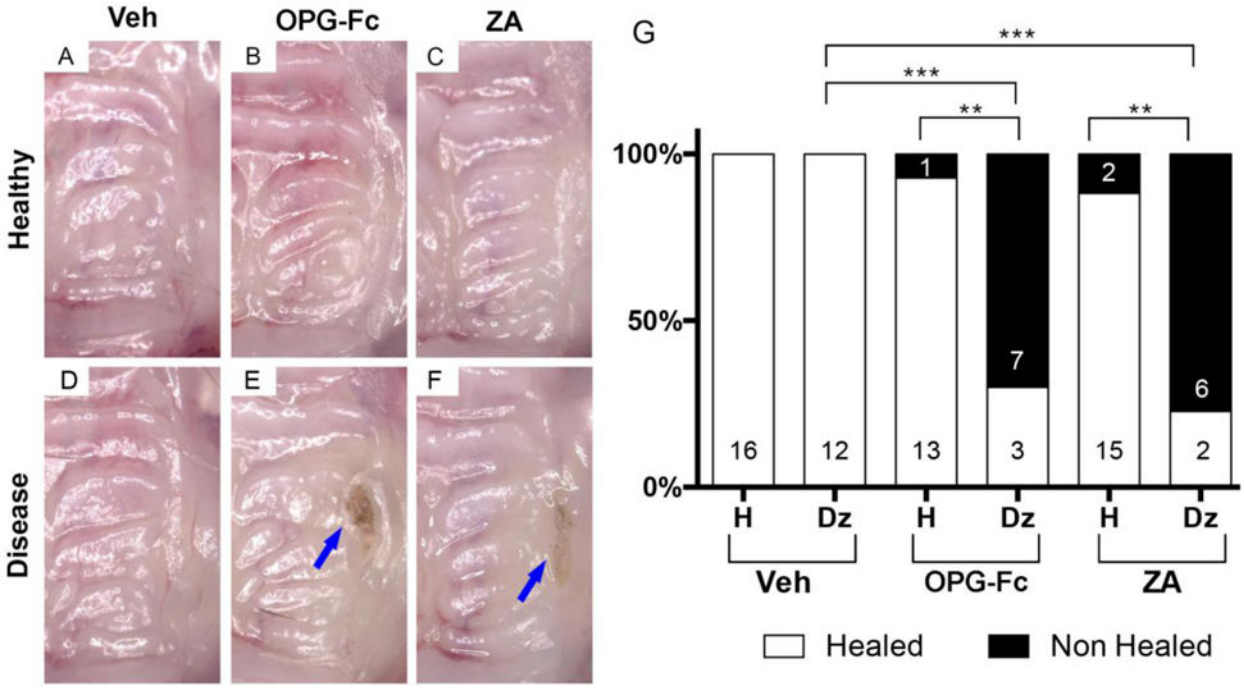

Figure 2. Visual assessment of mucosal healing of maxillary alveolar ridge after tooth extraction

(A–C) Maxillae in vehicle, OPG-Fc, and ZA groups after extraction of healthy teeth, respectively. (D–F) Maxillae in vehicle, OPG-Fc, and ZA groups after extraction of diseased teeth, respectively. Blue arrows point to areas of exposed bone. (G) Qualitative assessment of mucosal healing after healthy or diseased teeth in various treatment groups. *** Statistically significantly different, $p < 0.001$. ** Statistically significantly different, $p < 0.01$. Differences between groups were calculated by Fisher exact probability test.

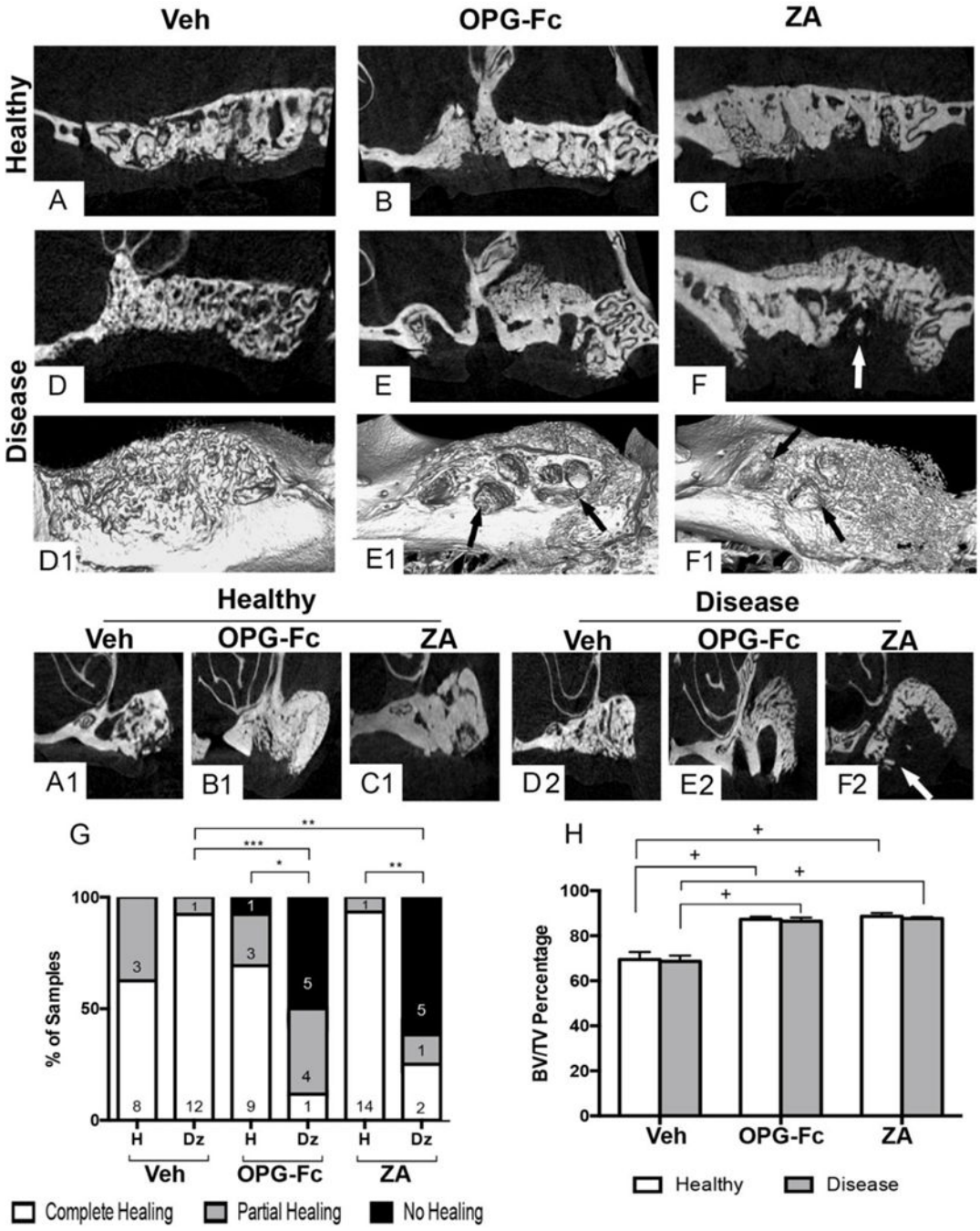

Figure 3. µCT assessment of the edentulous maxillary alveolar ridge and quantification of µCT findings

(A–F) Sagittal, (A1, B1, C1, D2, E2, F2) coronal views and (D1, E1, F1) 3D renderings of edentulous alveoli after extraction of healthy (A, B, C, and A1, B1, C1) or diseased (D, E, F, D1, E1, F1, D2, E2, F2) teeth in vehicle, OPG-Fc, or ZA groups. (G) Qualitative assessment of socket healing after extraction of healthy or diseased teeth in various treatment groups (H). Quantification of bone volume / tissue volume. + Statistically significantly different, $p < 0.0001$. ***Statistically significantly difference, $p < 0.001$. **Statistically significantly different, $p < 0.01$. *Statistically significantly different, $p < 0.05$. Differences between

groups for (G) were calculated by Fisher exact probability test. Differences among groups for (H) were calculated by two-way ANOVA and post-hoc Tukey's test for multiple comparisons. Data represent the mean ± SEM.

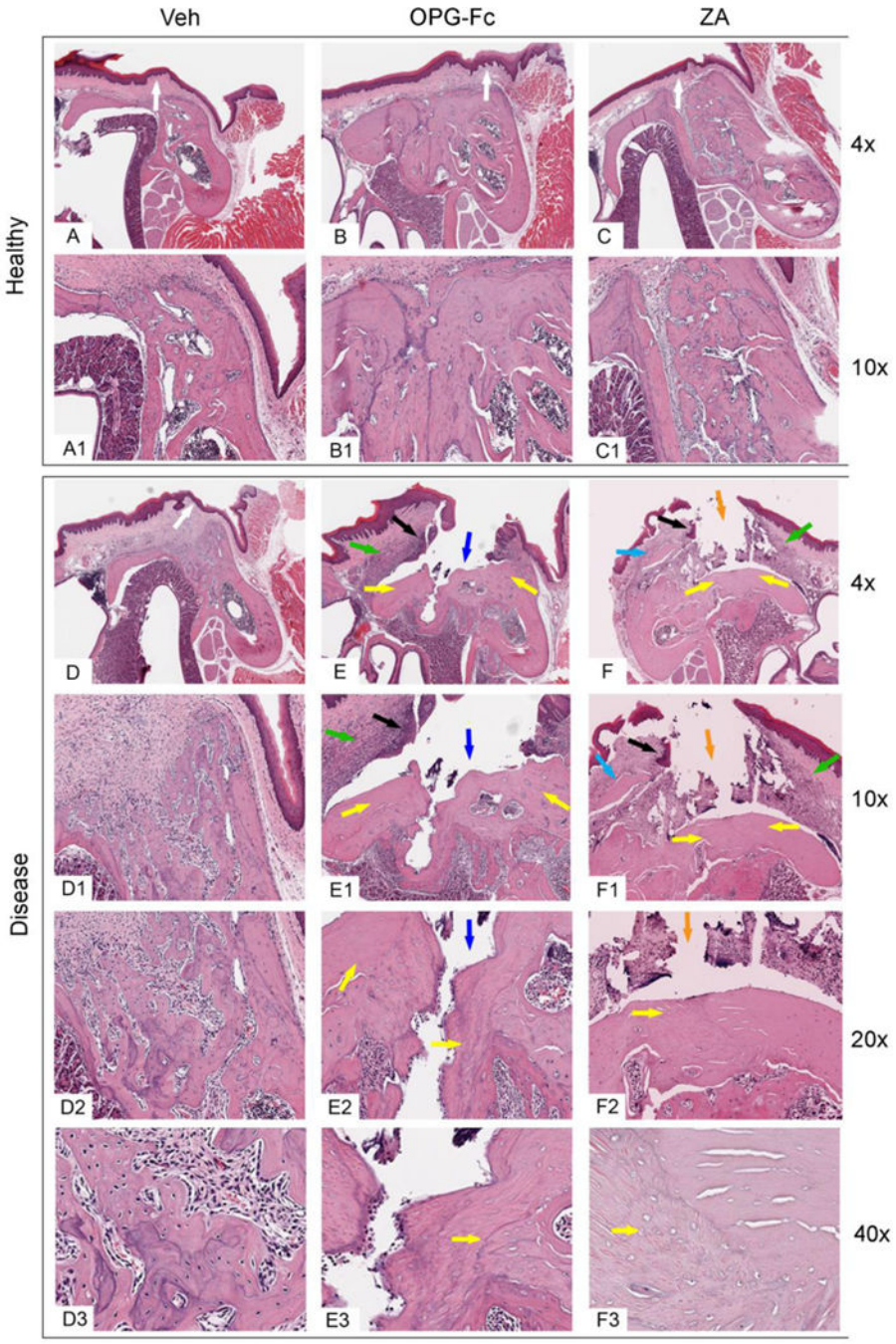

Figure 4. Representative H&E-stained images from maxillae of all groups

Alveolar ridge after extraction of (A, A1, B, B1, C, C1) healthy or (D, D1, D2, D3, E, E1, E2, E3, F, F1, F2, F3) diseased teeth of vehicle, OPG-Fc, and ZA groups, respectively, viewed at 4 ×(A, B, C, D, E, F), 10 × (A1, B1, C1, D1, E1, F1), 20 × (D2, E2, F2), or 40× (D3, E3, F3) magnification. White arrows point to normal epithelia lining, green arrows to inflammatory infiltrate, black arrows to epithelial migration, blue arrows to bone exposure, orange arrows to fragmented connective tissue, yellow arrows to areas of osteonecrosis, light blue arrows to sequestra.

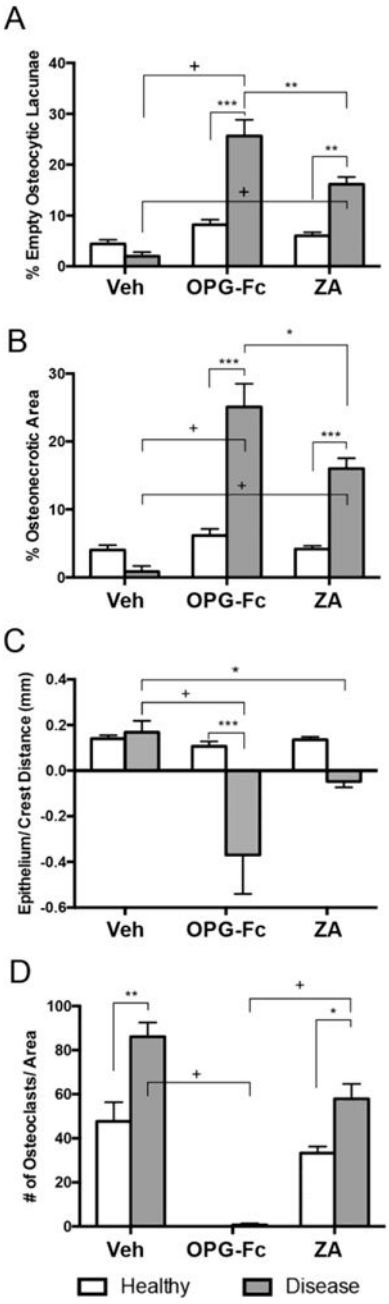

Figure 5. Quantification of the histologic findings

(A) percent empty osteolytic lacunae, (B) percentage of osteonecrotic area, (C) distance from lower point of epithelium to alveolar bone crest (D) number of TRAP+ cells per area + Statistically significantly different, $p < 0.0001$. ***Statistically significantly different, $p < 0.001$. **Statistically significantly different, $p < 0.01$. *Statistically significant different, $p < 0.05$. Differences among groups were calculated by two-way ANOVA and post-hoc Tukey's test for multiple comparisons. Data represent the mean ± SEM.